NeuroImage: Clinical 38 (2023) 103411

Contents lists available at ScienceDirect

NeuroImage: Clinical

journal homepage: www.elsevier.com/locate/ynicl

The potential for clinical application of automatic quantification of olfactory bulb volume in MRI scans using convolutional neural networks

Elbrich M. Postma [a,b,*], Julia M.H. Noothout [c,d], Wilbert M. Boek [b], Akshita Joshi [e], Theresa Herrmann [e], Thomas Hummel [e], Paul A.M. Smeets [a], Ivana Išgum [c,d,f], Sanne Boesveldt [a]

[a] Division of Human Nutrition and Health, Wageningen University & Research, Wageningen, The Netherlands
[b] Department of Otorhinolaryngology, Hospital Gelderse Vallei, Ede, The Netherlands
[c] Image Sciences Institute, University Medical Center Utrecht, Utrecht, The Netherlands
[d] Department of Biomedical Engineering and Physics, Amsterdam UMC – location AMC, University of Amsterdam, Amsterdam, The Netherlands
[e] Smell and Taste Clinic, Department of Otorhinolaryngology, TU Dresden, Dresden, Germany
[f] Department of Radiology and Nuclear Medicine, Amsterdam UMC – location AMC, University of Amsterdam, Amsterdam, The Netherlands

ARTICLE INFO

Keywords:
Olfactory loss
Deep learning
Convolutional neural networks
Segmentation
Olfactory bulb volume

ABSTRACT

The olfactory bulbs (OBs) play a key role in olfactory processing; their volume is important for diagnosis, prognosis and treatment of patients with olfactory loss. Until now, measurements of OB volumes have been limited to quantification of manually segmented OBs, which is a cumbersome task and makes evaluation of OB volumes in large scale clinical studies infeasible. Hence, the aim of this study was to evaluate the potential of our previously developed automatic OB segmentation method for application in clinical practice and to relate the results to clinical outcome measures.

To evaluate utilization potential of the automatic segmentation method, three data sets containing MR scans of patients with olfactory loss were included. Dataset 1 ($N = 66$) and 3 ($N = 181$) were collected at the Smell and Taste Center in Ede (NL) on a 3 T scanner; dataset 2 ($N = 42$) was collected at the Smell and Taste Clinic in Dresden (DE) on a 1.5 T scanner. To define the reference standard, manual annotation of the OBs was performed in Dataset 1 and 2. OBs were segmented with a method that employs two consecutive convolutional neural networks (CNNs) that the first localize the OBs in an MRI scan and subsequently segment them.

In Dataset 1 and 2, the method accurately segmented the OBs, resulting in a Dice coefficient above 0.7 and average symmetrical surface distance below 0.3 mm. Volumes determined from manual and automatic segmentations showed a strong correlation (Dataset 1: $r = 0.79$, $p < 0.001$; Dataset 2: $r = 0.72$, $p = 0.004$). In addition, the method was able to recognize the absence of an OB. In Dataset 3, OB volumes computed from automatic segmentations obtained with our method were related to clinical outcome measures, i.e. duration and etiology of olfactory loss, and olfactory ability. We found that OB volume was significantly related to age of the patient, duration and etiology of olfactory loss, and olfactory ability ($F(5, 172) = 11.348$, $p < 0.001$, $R^2 = 0.248$).

In conclusion, the results demonstrate that automatic segmentation of the OBs and subsequent computation of their volumes in MRI scans can be performed accurately and can be applied in clinical and research population studies. Automatic evaluation may lead to more insight in the role of OB volume in diagnosis, prognosis and treatment of olfactory loss.

1. Introduction

On a daily basis, humans are exposed to thousands of different odors. While smell plays an important role in daily life, 3% up to 20% of the general population exhibits olfactory loss (Boesveldt et al., 2017; Brämerson et al., 2004; Hoffman et al., 2016), which is often accompanied with complaints such as a diminished appetite, issues with daily safety, and a decreased quality of life (Boesveldt et al., 2017; Croy et al., 2014; Postma et al., 2020). Currently, a new population of patients is arising as olfactory loss is one of the symptoms of a Covid-19 infection (Parma et al., 2020). To be able to treat these patients, it is important to gain a better understanding of the human olfactory pathway.

* Corresponding author at: Division of Human Nutrition and Health, Wageningen University & Research, PO Box 17, 6700 AA Wageningen, The Netherlands.
E-mail address: elbrich.postma@wur.nl (E.M. Postma).

https://doi.org/10.1016/j.nicl.2023.103411
Received 16 March 2023; Accepted 17 April 2023
Available online 25 April 2023

The olfactory bulbs are the first recipient of odor signals in the human brain and process signals from the olfactory receptors cells in the nose and transmit them to the olfactory regions in the brain (Lundström et al., 2011). Volume of the olfactory bulbs has been associated with olfactory function (e.g. Buschhüter et al., 2008; Haehner, Rodewald, Gerber, & Hummel, 2008; Rombaux, Huart, Deggouj, Duprez, & Hummel, 2012). Moreover, the olfactory bulbs showed a reduced volume compared to healthy individuals in patients affected with olfactory loss (Han et al., 2017; Han et al., 2018; Shehata et al., 2018; Yao et al., 2018). Interestingly, olfactory bulb volume plays a role in prognosis for recovery in patients with olfactory loss: a larger olfactory bulb volume is related to a better recovery of smell ability (Rombaux et al., 2012). Moreover, olfactory training (Negoias et al., 2017) and medical treatment, like functional endoscopic sinus surgery (Gudziol et al., 2009; Sadeghi et al., 2015; Shehata et al., 2018) were both found to be related to an increase in olfactory bulb volume in patients with olfactory loss. Therefore, the volume of the olfactory bulbs -and their plasticity- may have important clinical implications for diagnosis, prognosis and treatment of patients with olfactory loss.

Various patient populations are affected by disease- and/or medication-related olfactory loss, such as patients with depression (Rottstaedt et al., 2018a; Rottstaedt, Weidner, Hummel, & Croy, 2018b), schizophrenia (Asal et al., 2018; Nguyen et al., 2011) and neurodegenerative diseases (Marin et al., 2018; Thomann et al., 2009). In these patients, reduced olfactory bulb volume was found compared to healthy controls, showing that studying the volume of this brain area and related outcome measures is clinically relevant. In addition, more research might lead to a better understanding of the role of the olfactory bulbs in relation to functioning of the brain during disease in general.

The olfactory bulbs are small structures, with a volume of more than 58 mm^3 in people under 45 years of age and a volume of more than 46 mm^3 in people older than 45 being considered as normal, (Buschhüter et al., 2008). A specialized MRI scan sequence is needed to visualize the olfactory bulbs. In the clinic, olfactory bulb volume is measured in these scans by manually tracing of the outlines of the bulbs in all slices that display them to compute their total volume (Hummel et al., 2015; Yousem et al., 1997). Such manual segmentation allows comparisons of (patient) groups within a study, follow-up of volume over time or comparison of relative differences in volumes between studies. However, while most work shows a high intra- and interrater reliability of repeated measurements within studies (see e.g. Gudziol et al., 2009; Hummel et al., 2015), differences may still be present between studies, making it problematic to compare absolute volumes between studies, or to establish cut-offs for olfactory bulb volume abnormalities applicable to different patient populations. Additionally, the current manual segmentation method is time consuming: on average, it takes 10 min per scan for a trained observer to segment the olfactory bulbs, which complicates clinical applications and hampers large scale studies.

Previously, other methods were developed to improve accuracy and speed of olfactory bulb volume measurements. Joshi et al. used the box-frame method. This method requires manual interaction (Joshi et al., 2020), while in recent years, deep learning techniques, and especially convolutional neural networks (CNNs), have become the method of choice for the automated analysis of medical images. CNNs analyze images through layers of convolutional filters to perform prediction (Litjens et al., 2017). These automated algorithms allow processing of large datasets in a short timeframe with increased reproducibility compared to manual analysis. Desser et al. (2021) and Estrada et al. (2021) both successfully developed automated methods to measure olfactory bulb volume. However, both studies used different methods and did not investigate the relation between the volumes measured by the automated methods and other clinical outcomes, like olfactory ability. In our previous work, we developed an automatic method for segmentation of the olfactory bulbs in MRI. The method first localizes the center of each OB using a CNN and defines region of interest by a bounding box that includes both OBs. Subsequently, the method analyzes the defined region of interest with another CNN to perform voxel-wise segmentation of the OBs (as described in detail in Noothout et al., 2021).

Table 1
Patient characteristics of patients included for the analysis for all datasets, including patients with congenital anosmia (mean ± SD or N (%)).

	Dataset 1 (N = 66)	Dataset 2 (N = 42)	Dataset 3 (N = 181)		
			Post-infectious (N = 68)	Chronic rhino-sinusitis (N = 61)	Trauma (N = 52)
Age (years)	59 ± 16.3	54 ± 15.4	60 ± 10.7	59 ± 12.7	49 ± 16.7
Men/women ratio	28/38	17/25	17/51	37/24	20/32
Duration of olfactory loss					
0–2 years	15 (23%)	24 (57%)	29 (43%)	11 (18%)	21 (40%)
2–5 years	16 (24%)	8 (19%)	20 (29%)	6 (10%)	18 (35%)
5–10 years	16 (24%)	3 (7%)	9 (13%)	22 (36%)	7 (13%)
> 10 years	15 (23%)	2 (5%)	10 (15%)	22 (36%)	6 (12%)
Whole life	4 (6%)	5 (12%)	0	0	0
Etiology of olfactory loss					
Idiopathic	22 (34%)	8 (19%)	0	0	0
Chronic rhinosinusitis	20 (30%)	0	0	61 (100%)	0
Post-infectious	12 (18%)	29 (69%)	68 (100%)	0	0
Trauma	4 (6%)	0	0	0	52 (100%)
Congenital	4 (6%)	5 (12%)	0	0	0
Other[a]	4 (6%)	0			0
Sniffin' Sticks score	16.1 ± 7.6[b]	17.0 ± 7.0	18.4 ± 6.7	15.5 ± 6.6 [b]	14.8 ± 6.6 [b]
Smell disorder					
Functional anosmia	34 (57%)	21 (50%)	28 (41%)	37 (62%)	31 (62%)
Hyposmia	23 (38%)	17 (40%)	39 (57%)	23 (38%)	18 (36%)
Normosmia	3 (5%)	4 (10%)	1 (2%)	0	1 (2%)

[a] = toxic/drugs (N = 3) and iatrogenic (N = 1).
[b] = could only be determined for 60/60/50 patients due to missing data.

The aim of the current study was to evaluate the potential of our previously developed automatic olfactory bulb segmentation method for application in clinical practice and in diverse studies. In the present study, we evaluated our method using three independent datasets. In two datasets, differing in acquisition parameters, we evaluated the performance of the method by comparing results with available manual reference annotations. In a third dataset, we related olfactory bulb volume computed solely from automatically obtained segmentations to clinical outcomes, i.e. duration and etiology of olfactory loss, and olfactory ability.

2. Data

2.1. Datasets

The method was evaluated using three different datasets including clinical patients with olfactory loss. In all datasets, patients' olfactory

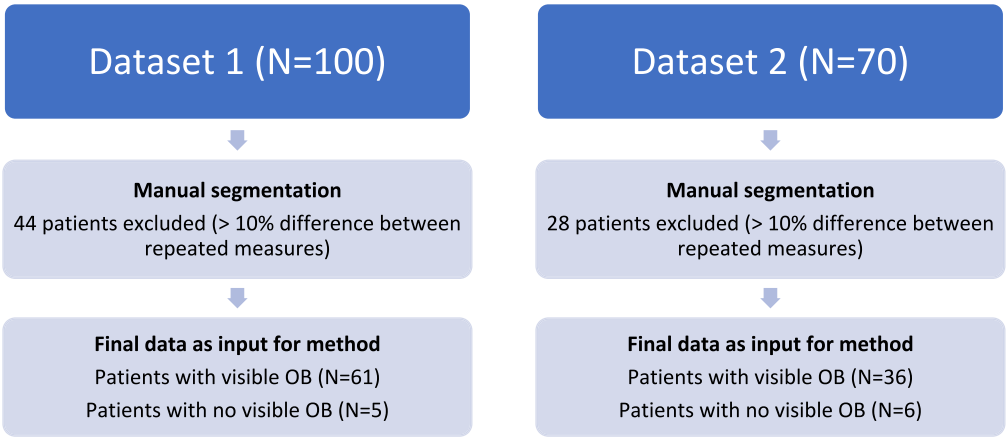

Fig. 1. Flowchart for Dataset 1 and 2, including input data and final data that was used as input for the method.

function was measured using the Sniffin' Sticks test (Hummel et al., 1996). The scores of this test (total range: 1–48; range in this study: 3.0–35.5) were used to categorize patients in one of the olfactory functioning groups: functional anosmia (TDI $\leq$ 16); hyposmia (16 $>$ TDI $<$ 30.75) or normosmia (TDI $\geq$ 30.75) (Oleszkiewicz et al., 2019). Characteristics of all patients are shown in Table 1.

2.1.1. Dataset 1

Dataset 1 was obtained from the Smell and Taste Center in Ede, The Netherlands. This dataset contained patients who visited the Smell and Taste Center between August 2015 and July 2017 and were diagnosed with olfactory loss. For this dataset, 100 patients were included as a random sample. All patients signed an informed consent on the use of their patient files for research and this study was approved by the review committee for scientific research of Hospital Gelderse Vallei, Ede, the Netherlands (BC/1703–143). MRI scans were acquired on a 3 T Siemens Magnetom Verio scanner (Siemens, Erlangen, Germany) with the use of a 32-channel head coil. To image the olfactory bulb, a coronal T_2-weighted 2D turbo spin-echo scan of 28 slices was made, using GRAPPA factor 2 (repetition time: 4630 ms; echo time: 153 ms; field of view: 205 $\times$ 256 mm; in-plane voxel size: 0.47 mm; slice thickness: 1.0 mm (no gap); 28 slices; flip angle = 145∘; total scan time: 4.30 min). In total, 61 patients with a visible olfactory bulb and 5 patients with no visible olfactory bulb were included for final analysis after manual segmentation of the olfactory bulbs (total N = 66).

2.1.2. Dataset 2

Dataset 2 was obtained from the Smell and Taste Center at the University Hospital Carl Gustav Carus in Dresden, Germany. This dataset contained 70 MRI scans of patients who were diagnosed with olfactory loss, and who signed an informed consent on the use of their medical records for research. MRI scans were acquired on a 1.5 T Siemens Verio scanner (Siemens, Erlangen, Germany) with the use of a 32-channel head coil. To image the olfactory bulb, a coronal T_2-weighted scan of 32 slices was made (repetition time: 2300 ms; echo time: 2.98 ms; field of view: 256 $\times$ 240 mm; in-plane voxel size: 0.47 mm; slice thickness: 1.2 mm (no gap); flip angle = 9∘; total scan time: 9.20 min). In total, 36 patients with a visible olfactory bulb and 6 patients with no visible olfactory bulb were included for final analysis after manual segmentation of the olfactory bulbs (total N = 42).

2.1.3. Dataset 3

Similar to Dataset 1, Dataset 3 was also obtained from the Smell and Taste Center in Ede, The Netherlands. This dataset contained 181 MRI scans of patients with clinically diagnosed olfactory loss based on three etiologies: post-infectious olfactory loss, olfactory loss due to chronic rhinosinusitis, or olfactory loss due to trauma. Patients visited the Smell and Taste center between July 2015 and February 2018 and signed an informed consent on the use of their patient files for research. MRI scans were made with the same acquisition settings as to those in Dataset 1.

2.2. Reference standard

To establish a reference standard, for every scan in Dataset 1 and 2, the left and right olfactory bulb were manually segmented and their volumes were subsequently computed.

For every scan, manual segmentation of the left and right olfactory bulb was obtained by performing planimetric manual contouring of each bulb in all slices according to a standardized protocol as described previously, following current practice for manual segmentations (Rombaux et al., 2009). Manual segmentation started with the selection of slices on which the olfactory bulbs were visible between the posterior parts of the eyeballs in the coronal plane. The first slice with a visually detectable olfactory bulb was used as the starting point of the manual segmentation. The contours of the olfactory bulbs were drawn manually in each successive slice. The sudden change in diameter at the beginning of the olfactory tract was used to define the end of the olfactory bulb (Rombaux et al., 2009; Yousem et al., 1997). After contouring, the volume of the left and right olfactory bulb in a scan was computed in mm^3 by multiplying the number of segmented voxels by the voxel size for each slice in which the olfactory bulb was visible.

Manual segmentation of the bulbs in Dataset 1 and 2 was performed by observers who were all trained following the same protocol, including data from 10 different patients, ranging from 'easy to segment' and 'difficult to segment'. In Dataset 1, manual segmentations were performed twice by one observer on different days. When the repeated segmentations differed more than 10% in volume from each other, a third segmentation was conducted to obtain two segmentations that differed<10%. In Dataset 2, manual segmentations were performed by two independent observers on different days. The observers were blinded to all patient characteristics. To minimize variability in both datasets for training of the algorithm, only two segmentations of the same bulb that differed $<$ 10% in volume were included. Based on this criterion, for the final dataset, 61 patients with a visible olfactory bulb from Dataset 1 and 36 patients with a visible olfactory bulb from Dataset 2 were included (Fig. 1). To perform the segmentation, for Dataset 1, MIPAV software (version 7.4.0, Centre for Information Technology, National Institutes of Health, Bethesda, Maryland, USA) was used, while for Dataset 2, AMIRA software (version 6.0, Department for Scientific Visualization, Zuse Institute Berlin (ZIB)) and AVIZO software (version 9.4, ThermoFisher Scientific, Waltham, Massachusetts, USA) were used. For Dataset 3, no manual reference segmentations were obtained.

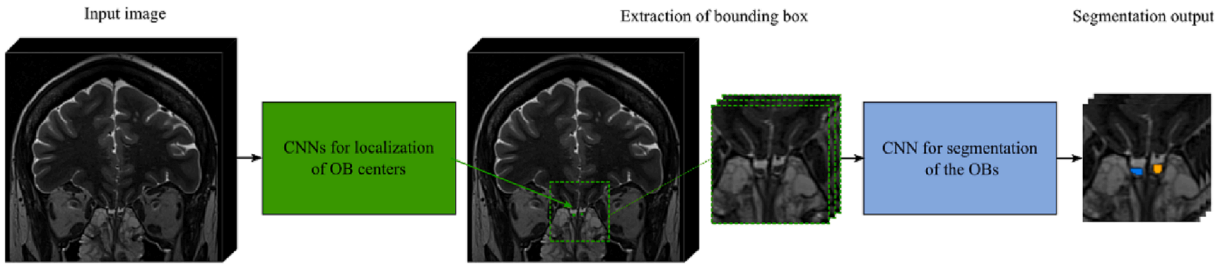

Fig. 2. Automatic segmentation of the olfactory bulbs in MRI scans using convolutional neural networks (CNNs). First, the center of each OB is localized. Subsequently, a region of interest (ROI) containing both olfactory bulbs is extracted and used as input for the segmentation of both olfactory bulbs to determine their volumes (figure derived from [Noothout et al., 2021], with permission).

3. Method

For automatic segmentation of the olfactory bulbs in MRI, we applied our previously developed method (Noothout et al., 2021). The method performs automatic segmentation of the olfactory bulbs in MRI scans in two consecutive steps. First, the center of each olfactory bulb is localized to define a region of interest (ROI) containing both bulbs. Subsequently, the ROI is analyzed to automatically segment the olfactory bulbs. After automatic segmentation, bulb volumes are determined from the obtained segmentations (see Fig. 2).

3.1. Automatic localization

Localization of the centers of the olfactory bulbs is performed using a landmark localization method performing a global-to-local analysis of images using CNNs (Noothout et al., 2020).

To obtain a reference location for the center of each olfactory bulb for training of the localization CNNs, the center of each manually segmented olfactory bulb was computed. For automatic localization of the olfactory bulb centers, one global and two specialized CNNs, i.e. one for the left and one for the right olfactory bulb, were trained. Both the global and local localization CNNs analyzed image patches and perform regression and classification tasks simultaneously. Hence, training was performed using a combined loss-function consisting of two parts. For the regression task, the mean absolute error was computed between the reference displacements and the regression output, while for the classification task, the binary cross-entropy between reference labels and the classification output was computed. CNNs were trained for 300,000 iterations using mini-batches containing 4 randomly sampled sub-images. During every iteration, the global CNN analyzed mini-batches containing sub-images of size 72x72x72 voxels, while specialized CNNs each analyzed mini-batches containing sub-images of size 16x16x16 voxels. Adam (Kingma & Ba, 2015) (lr = 0.001) was used to optimize network weights. During training, networks were evaluated on the validation set every 10,000 iterations. The best performing settings were defined as final parameter settings and used during testing.

3.2. Automatic segmentation

After localization, predicted center locations are used to define a region of interest (ROI) containing both bulbs. To ensure that the bulbs are completely contained within the ROI, the ROI contains all coronal slices of the MRI and has an in-plane size of 61x61 pixels. To automatically segment the olfactory bulbs, a CNN is trained to classify each pixel in the coronal slices of an ROI as left or right olfactory bulb, or background (Noothout et al., 2021).

For automatic segmentation of the olfactory bulbs, a segmentation CNN was trained during 80,000 iterations. During every iteration, the network analyzed a mini-batch containing 40 sub-images of size 35x35 pixels, of which the network classified the center 21x21 pixels. The Dice coefficient was used as loss-function and network weights were optimized using Adam (Kingma & Ba, 2015) (lr = 0.001). As an example of the output of the automatic segmentation method, individual results for 10 randomly selected patients are shown in Appendix A (Table A1).

To train the CNN to recognize the absence of an olfactory bulb, before training 5 and 6 MRI of patients without (visible) olfactory bulbs, originating from the respective centers, were added to Dataset 1 and 2, respectively.

4. Evaluation

Performance of the automatic segmentation method was evaluated for the localization and segmentation step separately, using Dataset 1 and 2. Dataset 3 was used for statistical analysis of automatically obtained segmentations and clinical outcome measures.

4.1. Evaluation of the automatic segmentation method

Manual reference segmentations were available for Dataset 1 and 2. Due to substantially different characteristics of the images in the two datasets, analysis was performed per set. Performance of the localization networks was evaluated by computing the Euclidean distance error between automatic and manual reference location of the center of each olfactory. Evaluation of the segmentation network was performed by computing the Dice coefficient to evaluate the overlap between automatic and manual segmentations, and the average symmetrical surface distance (ASSD) in millimeters between automatic and manual segmentations to evaluate automatic segmentation along the bulbs surface. To improve performance of the automatic segmentation CNN on Dataset 2, transfer learning was applied by initializing the segmentation CNN with the weights of the CNN trained only on Dataset 1 and subsequent training of the CNN with the training set of Dataset 2 during 40,000 iterations.

The correlation between olfactory bulb volumes computed from the manual segmentations and the automatic segmentations was investigated by performing Spearman's correlation in IBM SPSS Statistics (version 25). Furthermore, because scans can contain non-visible olfactory bulbs, as there are patients who are born with a very small or even invisible olfactory bulbs (Abolmaali et al., 2002; Karstensen et al., 2018), the ability of the network to recognize the *absence* of an olfactory bulb was evaluated by using available scans of patients with no visible olfactory bulbs.

4.2. Relating olfactory bulb volume to clinical outcome measures

To investigate how automatically determined OB volumes based on the segmentations from the CNN are related to clinical outcome measures, i.e. olfactory ability and etiology and duration of olfactory loss, olfactory bulb volumes in Dataset 3 were computed from the automatic segmentations. Subsequently, differences in olfactory bulb volume between etiologies and durations of olfactory loss were calculated using a Kruskal-Wallis test. The relation between objective smell function as

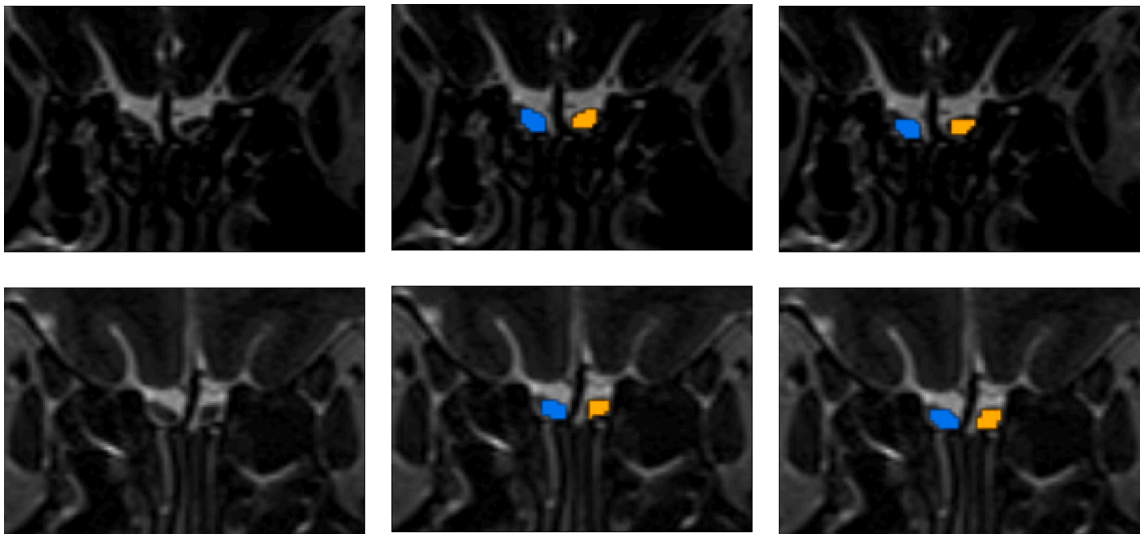

Fig. 3. Automatic segmentation of the left (orange) and right (blue) olfactory bulb in two MRI scans (rows). The first column shows a coronal slice of the image, cropped for visualization purposes. The middle column shows the automatic segmentation result, obtained with the method while the last column shows the reference segmentation (manual segmentation). (For interpretation of the references to colour in this figure legend, the reader is referred to the web version of this article.)

Fig. 4. Automatic segmentation of the right (yellow) olfactory bulb. The left column shows the posterior coronal slice, where the cut-off needs to be made between the olfactory bulb and the olfactory nerve, cropped for visualization purposes. The middle column shows the automatic segmentation result, obtained with the method while the last column shows the reference segmentation (manual segmentation).

measured with the Sniffin' Sticks test and olfactory bulb volume was tested using Spearman's correlations. Additionally, a multiple linear regression was performed to investigate the relation between olfactory bulb volume and age, sex, etiology and duration of olfactory loss, and olfactory ability. All tests were performed in IBM SPSS Statistics (version 25).

5. Experiments and results

Before experiments, Dataset 1 was randomly divided into a training dataset (43 MRI scans), a validation dataset (2 MRI scans), and a hold-out test dataset (21 MRI scans). In the training and test set, three and two scans without clearly visible olfactory bulbs were present, respectively. Dataset 2 was also randomly divided into a training set (20 MRI scans), a validation set (2 MRI scans) and a hold-out test set (20 MRI scans). In the test set, six scans without clearly visible olfactory bulbs were present. Dataset 3 was solely used as a hold-out test set (181 MRI scans). Overall, training and validation sets were used to develop the method while hold-out test sets were not used during method development in any way.

5.1. Automatic segmentation of visible olfactory bulbs

5.1.1. Dataset 1

The localization CNNs and the segmentation CNN were trained using training scans from Dataset 1. Automatic localization of the olfactory bulb centers in the test set of Dataset 1 resulted in an average Euclidian distance error between reference and automatically obtained locations of 1.24 ± 0.84 mm for the left, and 1.40 ± 1.21 mm for the right olfactory bulb. Subsequent automatic segmentation of the olfactory bulbs resulted in an average Dice coefficient and ASSD of 0.79 ± 0.13 and 0.23 ± 0.31 mm for the left olfactory bulb, respectively, and an average Dice coefficient and ASSD of 0.82 ± 0.10 and 0.17 ± 0.18 mm for the right olfactory bulb, respectively. Fig. 3 shows segmentation results obtained on two images from the test set, for which the method obtained Dice coefficients of 0.89 and 0.90 for segmentation of the left bulbs, and 0.88 and 0.91 for segmentation of the right bulbs. Total time needed for the localization and segmentation per MRI scan was 0.20 s. For illustration purposes, we added an example of olfactory bulb volume obtained by automatic segmentation at the posterior coronal slice, where the cut-off needs to be made between the olfactory bulb and the olfactory nerve (Fig. 4).Subsequently, olfactory bulb volumes were calculated from the automatic segmentation and correlated with the volumes calculated from the manual measurements (Table 2). The

Table 2
Mean ± SD volume of the left and right OB in mm^3 measured with the manual measurements and the volumes based on the segmentations from the CNN in the test set of Dataset 1 (N = 19).

	Manual measurements	Automated measurements	Correlation
Volume left olfactory bulb	43.6 ± 12.90	40.0 ± 15.04	r = 0.92, p < 0.001
Volume right olfactory bulb	47.3 ± 12.37	42.2 ± 10.32	r = 0.47, p = 0.04
Total volume olfactory bulbs	90.0 ± 24.79	80.2 ± 20.83	r = 0.79, p < 0.001

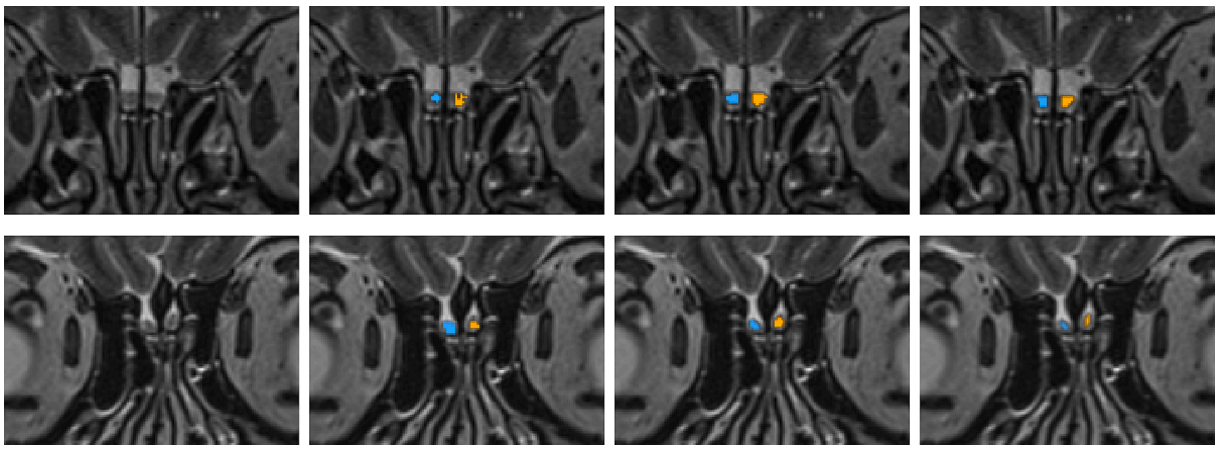

Fig. 5. Automatic segmentation of the left (orange) and right (blue) olfactory bulb in two MRI scans (rows). The first column shows an axial slice of the image, cropped for visualization purposes. The second and third column show the segmentation results, obtained with the segmentation CNN trained with only Dataset 1 and with additional training with Dataset 2, respectively, while the last column shows the reference segmentation. Dice coefficients improved from 0.64 to 0.75 (first row), and from 0.42 to 0.62 (second row) for the left olfactory bulb, while for the right olfactory bulb Dice coefficients improved from 0.74 to 0.83 (first row), and from 0.54 to 0.65 (second row). (For interpretation of the references to colour in this figure legend, the reader is referred to the web version of this article.)

Table 3
Mean ± SD volume of the left and right OB in mm^3 measured with the manual measurements and the volumes based on the segmentations from the CNN in the test set of Dataset 2 (N = 14).

	Manual measurements	Automated measurements	Correlation
Volume left olfactory bulb	21.8 ± 9.18	27.3 ± 9.64	r = 0.80, p = 0.001
Volume right olfactory bulb	22.8 ± 9.27	27.5 ± 7.85	r = 0.76, p = 0.002
Total volume olfactory bulbs	44.5 ± 17.58	54.8 ± 15.57	r = 0.72, p = 0.004

average absolute volumetric difference was 7.49 ± 5.42 mm^3 for the left olfactory bulb and 7.88 ± 9.74 mm^3 for the right olfactory bulb. All volumes showed a significantly moderate to strong positive correlation between results from the manual measurements and the volumes calculated based on the segmentations from the CNNs. A Bland-Altman plot for these results is added in Appendix A (Figure A1).

5.1.2. Dataset 2

The previously trained localization CNNs were also evaluated on Dataset 2, which had different MRI acquisition parameters compared to Dataset 1. On average, automatic localization of the center of the left and right olfactory bulb in the test set showed a Euclidean distance error of 1.81 ± 1.55 and 2.15 ± 1.38 mm. Even though distance errors were slightly higher compared to those for Dataset 1, ROIs could still be successfully extracted and no olfactory bulb was left out.

Subsequent automatic segmentation of the olfactory bulbs after additional training with Dataset 2 resulted in an average an average Dice coefficient and ASSD of 0.72 ± 0.13 and 0.26 ± 0.29 mm for the left olfactory bulb, respectively, and an average Dice coefficient and ASSD of 0.74 ± 0.10 and 0.23 ± 0.19 mm for the right olfactory bulb, respectively. Fig. 5 shows segmentation results obtained on two images from the test set with the method trained with only Dataset 1 and with the method trained additionally with Dataset 2. For both images, segmentation results improved when additional training with Dataset 2 was performed.

Subsequently, olfactory bulb volumes were calculated for the segmentations obtained with the CNN additionally trained with Dataset 2 and correlated with the volumes calculated from the manual measurements (Table 3). All volumes showed a significant moderate to strong positive correlation. A Bland-Altman plot for these results is added in Appendix A (Figure A1).

Table 4
Mean ± SD accuracy measures for left and right olfactory bulb volume measurements by the segmentation network for Dataset 1 (N = 2) and 2 (N = 6); both datasets included only patients with no visually detectable olfactory bulb.

Training method	Test set	Abs. vol. difference left	Abs. vol difference right
DS 1	No bulb DS 1	1.53 ± 1.53	3.74 ± 3.74
DS 1	No bulb DS 2	2.24 ± 1.47	2.55 ± 3.72
DS 1 – DS 2	No bulb DS 2	2.86 ± 1.72	1.67 ± 1.94

DS = dataset; DS 1 – DS 2 = trained on Dataset 1 and additionally on Dataset 2; abs. vol. difference = absolute volumetric difference in mm^3.

5.2. Automatic segmentation of non-visible olfactory bulbs

Clinical populations with olfactory loss also include patients who have no visible olfactory bulbs, e.g. patients with congenital anosmia (Abolmaali et al., 2002; Karstensen et al., 2018). Therefore, the ability of the network to recognize the *absence* of an olfactory bulb was evaluated by using available scans of patients with no visible olfactory bulbs of Dataset 1 and 2 (Table 4). Here, the Dice coefficient and ASSD could not be calculated as manual segmentations were -by definition- not possible in these scans. On average, segmentation results yielded volumes smaller than 4 mm^3.

Table 5
Mean ± SD volume of the left and right OB in mm^3 based on the segmentations from the CNN for the different etiologies and correlation between total volume and Sniffin' Sticks score in MRI of Dataset 3.

	Post-infectious (N = 68)	Chronic rhinosinusitis (N = 61)	Trauma (N = 52)
Total volume olfactory bulbs	73.5 ± 25.61[a]	79.5 ± 29.96[a]	37.4 ± 29.85[b]
Correlation volume – olfactory ability	r = 0.15, p = 0.23	r = -0.03, p = 0.81	r = 0.50, p < 0.001

Different letters indicate significant differences between groups ($p < 0.05$).

5.3. Relating olfactory bulb volume to clinical outcome measures

Because image acquisition parameters were the same as those from Dataset 1 (Section 2.1.3), the method trained with Dataset 1 was used to automatically segment the olfactory bulbs in MRI of Dataset 3. Subsequently, volumes of the olfactory bulbs were computed using the automatic segmentations and related to clinical outcome measures, i.e. olfactory ability, and etiology and duration of olfactory loss. Results showed that there was a significant effect of etiology of olfactory loss on total olfactory bulb volume ($\chi^2(2) = 49.623$, $p < 0.001$). Total volume was significantly smaller in patients with olfactory loss due to trauma compared to patients with olfactory loss due to chronic rhinosinusitis ($p < 0.001$) or patients with post-infectious olfactory loss ($p < 0.001$) (Table 5). In addition, there was a significant effect of duration of olfactory loss on total olfactory bulb volume ($\chi^2(3) = 11.311$, $p = 0.01$): pairwise comparisons only showed a significant difference in volume between patients with olfactory loss for 2–5 years and for 5–10 years ($p = 0.02$).

In the total population, there was a significantly moderate positive correlation between olfactory ability and olfactory bulb volume ($r = 0.21$, $p = 0.006$). When looking at the etiology subgroups separately, there was a significant correlation between total volume and olfactory ability for patients with olfactory loss due to head trauma ($r = 0.50$, $p < 0.001$; Table 5), but not for the other etiologies. For comparison reasons, we also correlated olfactory ability with olfactory bulb volume for the patients in dataset 1 and 2 using Spearman's rank correlations. There was no correlation between olfactory ability and both measurements of olfactory bulb volume (see Table A2 in Appendix A).

A multiple regression model was used to predict olfactory bulb volume from age, sex, and duration and etiology of olfactory loss. This model showed that these variables significantly predicted olfactory bulb volume ($F(5, 172) = 11.348$, $p < 0.001$, $R^2 = 0.248$). Of these variables, sex (beta = -0.166, $p = 0.02$), duration (beta = 0.178, $p = 0.03$), etiology (beta = -0.406, $p < 0.001$) and olfactory ability (beta = 0.174, $p = 0.01$) significantly contributed to the prediction. Average olfactory bulb volume in women was 11.28 mm^3 smaller than in men. For the subgroups of duration, there was an average decrease of olfactory bulb volume of 5.20 mm^3 for a longer duration of olfactory loss. For etiologies of olfactory loss, the biggest volume was found in the post-infectious patients, followed by chronic rhinosinusitis and trauma patients, with a decrease in olfactory bulb volume of 16.76 mm^3 per group. Lastly, an increased olfactory ability was related to an increased olfactory bulb volume of 0.86 mm^3.

6. Discussion

In this study, we evaluated the potential of our previously developed automatic olfactory bulb segmentation method for clinical measurements of olfactory bulb volume. We have shown that our method was able to accurately segment olfactory bulbs in MRI scans differing in acquisition parameters and that volumes computed from automatic segmentations were moderately to highly correlated with those computed from manual segmentations. These results are similar to the results of previously developed methods. Moreover, the method was able to detect the absence of an olfactory bulb. Additionally, we have shown that volumes computed from automatically obtained segmentations are related to clinical outcome measures such as duration and etiology of olfactory loss, indicating that the use of our automated method to segment the olfactory bulbs has potential for clinical applications, e.g. in various populations of patients with olfactory loss.

We evaluated our method using three datasets acquired on different MRI scanners. For Dataset 1, automatic segmentation of the olfactory bulbs resulted in an average Dice coefficient above 0.8 and an ASSD below 0.24 mm. For Dataset 2, additional training of the segmentation CNN resulted in an average Dice coefficient of above 0.72 and an ASSD below 0.26 mm, which is slightly worse compared to the performance on Dataset 1. Reasons for this could be a larger slice thickness for scans in Dataset 2 than in Dataset 1 and the limited sizes of the datasets. In a smaller sample, interindividual variability, associated with a patient population, can have a large impact on the final result. However, the Bland-Altman plot showed only one result that exceeded the upper 95% CI. Additionally, there were differences in image acquisition parameters between datasets. Scans from Dataset 2 were made on a 1.5 T MRI scanner. Therefore, image acquisition time for Dataset 2 was longer than for Dataset 1 (3 T), which might have led to motion artefacts, also caused by the interleaved scanning sequence that was used. Future work should focus on training a single CNN using heterogeneous training data representing diverse populations and comprised of scans made with different scanners and different image acquisition protocols to make the method more robust., This will make the method applicable to quantification of olfactory bulb volume for a wider variety of scans with diverse acquisition parameters. Nevertheless, our results show that the results based on the noisier scans obtained on a 1.5 T scanner were still accurate once additional training was performed.

Dataset 1 and 2 also included patients who did not have an olfactory bulb due to congenital anosmia and patients who suffered from olfactory loss after head trauma and did not have a visible olfactory bulb, probably due to lesions caused by the head trauma (Lötsch et al., 2016). The method was able to successfully detect the *absence* of an olfactory bulb in these scans. In these scans, on average, segmentation results yielded volumes smaller than 4 mm^3. This volume is unlikely in bulbs visually detectable on MRI and suggests that the method can be applied to the full range of olfactory bulb volumes seen in clinical practice.

Olfactory bulb volume can be an important indicator for prognosis of patients with olfactory loss (Rombaux et al., 2012). Fast and reliable measures of olfactory bulb volume in relation to other clinical outcome measures are therefore of importance for daily health care. While we found a strong correlation between both measurements for the left OB, the correlation between volumes for the right OB was lower. A similar correlation for both side olfactory bulbs would be expected. However, in clinical patient data, we often see that there is a difference in volume and demarcation between the left and right side of the olfactory bulb, for example due to trauma or to chronic infections in the nose. In our datasets, these etiologies were present among the included patients. This could have influenced the correlations for each bulb. Using Dataset 3, we showed that the volumes can be related to clinical outcome measures, which is in line with previous studies in patients, that also found differences in volume between different etiologies of olfactory loss (Thomas Hummel et al., 2015; Yildirim et al., 2020), a decrease of volume in patients with a longer duration of olfactory loss (Yao et al., 2018), and a relation between volume and olfactory function (Haehner et al., 2008; Thomas Hummel et al., 2015). Moreover, we found a difference in volume between women and men, while there was no significant relation between age and olfactory bulb volume, which is in line with previous findings in healthy participants (Buschhüter et al., 2008) and patients (Hummel et al., 2015).

We consider the use of our method as described in the current study as a proof of principle that the use of automated assessment of olfactory bulb volume in clinical settings is feasible after further training of the CNNs. Our results show that this method can accurately perform measurements of olfactory bulb volume in a much faster manner than manual measurements (0.2 s compared to 10 min), while the reliability of the measurements is independent from individual observers. Altogether this indicates the potential for applying this automated method in clinical settings in which olfactory bulb volume is relevant, for example in patients with depression (Rottstaedt et al., 2018a; Rottstaedt, Weidner, Hummel, & Croy, 2018b), schizophrenia (Asal et al., 2018; Nguyen et al., 2011) or neurodegenerative diseases (Marin et al., 2018; Thomann et al., 2009). However, olfactory bulb volume is not only relevant for diseases that are primarily related to the brain; there is also evidence that it can be of clinical relevance in other patients, such as patients with obstructive sleep apnea (Doğan et al., 2020), patients with obesity

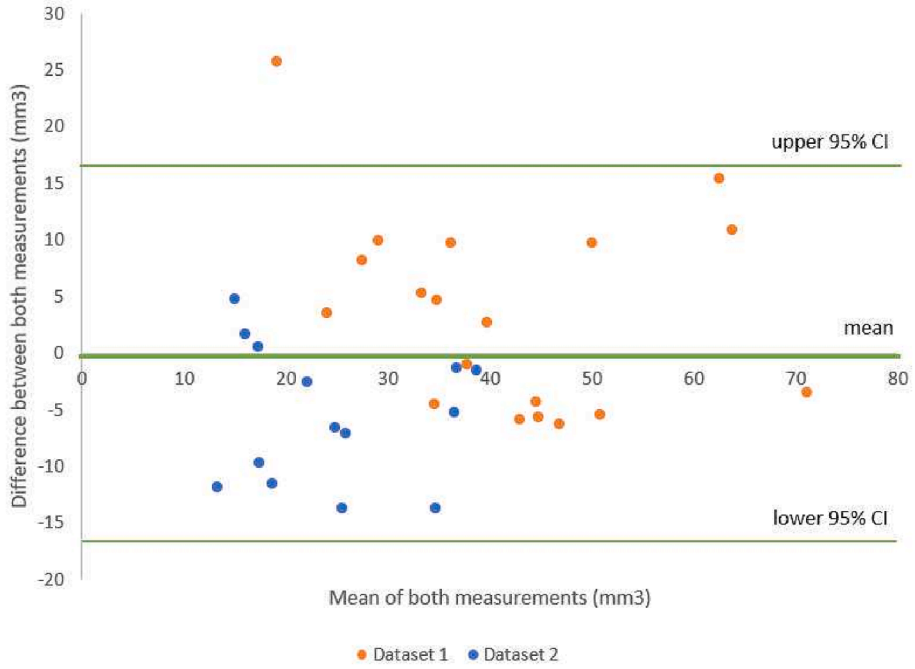

Fig. A1. Bland-Altman plot, showing the average difference in measurements between both measurements.

(Karaoglan & Colakoglu Er, 2020; Poessel et al., 2020). In addition, current studies showed that olfactory loss due to a COVID-19 infection can lead to atrophy of the olfactory bulb volume (Chiu et al., 2021; Tsivgoulis et al., 2021). Therefore, this method will be widely applicable in the future.

Another clinical application would be the follow-up of olfactory bulb volume over time. These measurements can be applied to follow progression of disease over time, or for instance to monitor the effect of treatment for olfactory loss, like olfactory training, on olfactory bulb volume. Moreover, this would allow further research on olfactory bulb volume in relation to disease. In neurodegenerative diseases like Parkinson's disease of Alzheimer's disease, changes in olfactory ability can be an early signal for development of disease (Attems et al., 2015; Marin et al., 2018). Further investigations on changes in olfactory bulb volume may give more insight in the role of changes in olfactory bulb volume in detection of neurodegenerative diseases at an early stage. In the future, this might increase the possibilities for an early start of treatment (Fullard et al., 2017; Kumar & Singh, 2015).

Our current results are based on training the segmentation CNN with images for which manual reference segmentations were available. While previous studies show that this can yield reliable results based on inter- and intra-rater comparisons (Huart et al., 2019; Thomas Hummel et al., 2015), surprisingly little is known about how these manual segmentations relate to the *actual* volume of the olfactory bulb. In this study, manual segmentation was considered as the approximate ground truth. To determine how measurements of olfactory bulb volume in MRI scans relate to actual volume, ground truth should be measured. This would, for example, be possible by using post-mortem data. Implementing results from such ground truth measurements could be applied to improve manual measurements. Training the CNNs on these improved measurements might further increase accuracy of the automatic segmentation.

Results showed that the segmentations produced by our method can be used to calculate olfactory bulb volume in patients exhibiting olfactory loss, and can be extended to other patients with disease-related olfactory loss. As there are many individual differences in volume of the olfactory bulb, for example between men and women (Buschhüter et al., 2008; Rombaux et al., 2009) or due to ageing (Yousem et al., 1998), it is important to train the CNNs on a broad sample of patients, including multiple patients populations, as well as on a sample of healthy individuals to obtain absolute normative data. Therefore, this is a promising proof of principle on a limited amount of data. To further validate and refine the method, we aim to expand our dataset with additional MRI data of various patient groups and healthy individuals for which manual segmentation of olfactory bulb volume have been performed. By this, we will increase the variability of the dataset with which the CNNs are trained, which will enable the use of our CNNs in different settings for research and in daily practice. Moreover, this allows the investigation of total brain volume as determinant of olfactory bulb volume, since total brain volume affects grey matter volume (Lüders et al., 2002). Described software will be available to other researchers and health care professionals upon request at https://grand-challenge.org/algorithms/automatic-olfactory-bulb-segmentation-in-mri/.

7. Conclusion

In this study we demonstrated that the use of our automatic olfactory bulb segmentation method is accurate and fast, and that the results relate to clinical outcome parameters. This approach may facilitate the use of olfactory bulb volume measurements in clinical practice for patient populations with olfactory loss to improve diagnosis, prognosis and inform treatment options.

Funding

This research was partly funded by an Aspasia grant of the Netherlands Organization for Scientific Research (NWO; 015.013.052), awarded to SB, and is part of the research program Deep Learning for Medical Image Analysis with project number P15-26, funded by the Dutch Technology Foundation with participation of Philips Healthcare.

Declaration of Competing Interest

The authors declare that they have no known competing financial interests or personal relationships that could have appeared to influence the work reported in this paper.

Table A1
Individual data for 10 randomly selected patients from Dataset 1 and Dataset 2.

DS	Volume left		Volume right		Total volume		Sniffin' Sticks score	Etiology	Difference between measurements (total volume)	Mean of both measurements (total volume)
	Manual	Automated	Manual	Automated	Manual	Automated				
1	43.73	50.10	51.20	51.86	94.92	101.95	21.00	Post-infectious	−7.03	98.44
2	20.8	23.47	17.40	12.66	38.23	36.12	17.00	Post-infectious	2.11	37.18
2	36,12	37,44	37,71	35,86	73,83	73,30	15.75	Idiopathic	0.53	73.56
1	41.97	47.68	43.07	43.07	85.03	90.75	18.00	Idiopathic	1.76	72.07
1	42.41	46.80	40.87	46.14	83.28	92.94	11.50	Post-infectious	−9.67	88.11
2	12.92	24.52	11.87	17.14	24.79	41.66	14.00	Post-infectious	−16.88	33.22
1	31.64	23.51	35.38	38.67	67.02	62.18	9.00	Idiopathic	4.83	64.60
1	37.13	32.52	40.43	38.23	77.56	70.75	8.00	Idiopathic	6.81	74.16
2	17.67	17.14	19.51	21.62	37.18	38.76	24.50	Post-infectious	−1.58	37.97
1	32.30	36.91	39.11	52.95	71.41	89.87	10.00	Chronic rhinosinusitis	−18.46	80.64

Table A2
Correlations between total volume of the olfactory bulb and olfactory ability for manual measurements and automated measurements (including patients from dataset 1 and 2, N = 33 for all correlations).

	Manual measurements	Automated measurements
Olfactory ability	r = -0.10, p = 0.58	r = -0.06, p = 0.74

Data availability

Data will be made available on request.

Acknowledgments

The use of the 3 T MRI facility has been made possible by Wageningen University & Research Shared Research Facilities. We thank all MRI technicians at Hospital Gelderse Vallei for their help in conducting the MRI scans of the Dutch patients and in particular Arjen Riemsma for his help with implementing the scan sequence. Additionally, we thank Lisette van Amerongen for her help in performing the manual segmentations of the scans in Dataset 1.

Appendix 1 Additional data and analyses

References

Abolmaali, N.D., Hietschold, V., Vogl, T.J., Hu, K.-B., Hummel, T., 2002. MR Evaluation in Patients with Isolated Anosmia Since Birth or Early Childhood. Am J Neuroradiol 23, 157–163.

Asal, N., Bayar Muluk, N., Inal, M., Şahan, M.H., Doğan, A., Buturak, S.V., 2018. Olfactory bulbus volume and olfactory sulcus depth in psychotic patients and patients with anxiety disorder/depression. Eur. Arch. Otorhinolaryngol. 275 (12), 3017–3024. https://doi.org/10.1007/s00405-018-5187-x.

Attems, J., Walker, L., Jellinger, K.A., 2015. Olfaction and Aging: A Mini-Review. Gerontology 61, 485–490. https://doi.org/10.1159/000381619.

Boesveldt, S., Postma, E.M., Boak, D., Welge-Luessen, A., Schöpf, V., Mainland, J.D., Martens, J., Ngai, J., Duffy, V.B., 2017. Anosmia-A clinical review. Chem. Senses 42 (7), 513–523. https://doi.org/10.1093/chemse/bjx025.

Brämerson, A., Johansson, L., Ek, L., Nordin, S., Bende, M., 2004. Prevalence of Olfactory Dysfunction: The Skövde Population-Based Study. Laryngoscope 114 (3), 733–737. https://doi.org/10.1097/00005537-200404000-00026.

Buschhüter, D., Smitka, M., Puschmann, S., Gerber, J., Witt, M., Abolmaali, N., Hummel., T., 2008. Correlation between olfactory bulb volume and olfactory function. Neuroimage 42, 498–502. https://doi.org/10.1016/j.neuroimage.2008.05.004.

Chiu, A., Fischbein, N., Wintermark, M., Zaharchuk, G., Yun, P.T., Zeineh, M., 2021. COVID-19-induced anosmia associated with olfactory bulb atrophy. Neuroradiology 63 (1), 147–148. https://doi.org/10.1007/s00234-020-02554-1.

Croy, I., Hoffmann, H., Philpott, C., Rombaux, P., Welge-Luessen, A., Vodicka, J., Konstantinidis, I., Morera, E., Hummel, T., 2014. Retronasal testing of olfactory function: an investigation and comparison in seven countries. Eur Arch Otorhinolaryngol 271 (5), 1087–1095. https://doi.org/10.1007/s00405-013-2684-9.

Desser, D., Assunção, F., Yan, X., Alves, V., Fernandes, H.M., Hummel, T., 2021. Automatic Segmentation of the Olfactory Bulb. Brain Sci. 11, 1141. https://doi.org/10.3390/brainsci11091141.

Doğan, A., Bayar Muluk, N., Şahin, H., 2020. Olfactory Bulb Volume and Olfactory Sulcus Depth in Patients With OSA: An MRI Evaluation. Ear Nose Throat J. 99 (7), 442–447. https://doi.org/10.1177/0145561319881571.

Estrada, S., Lu, R., Diers, K., Zeng, W., Ehses, P., Stöcker, T., Breteler, M., Reuter, M., 2021. Automated olfactory bulb segmentation on high resolutional T2-weighted MRI. Neuroimage 242, 118464. https://doi.org/10.1016/j.neuroimage.2021.118464.

Fullard, M.E., Morley, J.F., Duda, J.E., 2017. Olfactory Dysfunction as an Early Biomarker in Parkinson ' s Disease. Neurosci. Bull. 33 (5), 515–525. https://doi.org/10.1007/s12264-017-0170-x.

Gudziol, V., Buschhüter, D., Abolmaali, N., Gerber, J., Rombaux, P., Hummel, T., 2009. Increasing olfactory bulb volume due to treatment of chronic rhinosinusitis-a longitudinal study. Brain 132 (11), 3096–3101. https://doi.org/10.1093/brain/awp243.

Haehner, A., Rodewald, A., Gerber, J., Hummel, T., 2008. Correlation of Olfactory Function With Changes in the Volume of the Human Olfactory Bulb. Arch Otolaryngol Head Neck Surg 134 (6), 621–624. https://doi.org/10.1001/archotol.134.6.621.

Han, P., Whitcroft, K., Fischer, J., Gerber, J., Cuevas, M., Andrews, P., Hummel, T., 2017. Olfactory brain gray matter volume reduction in patients with chronic rhinosinusitis. International Forum of Allergy & Rhinology 7 (6), 551–556. https://doi.org/10.1002/alr.21922.

Han, P., Winkler, N., Hummel, C., Hähner, A., Gerber, J., Hummel, T., 2018. Alterations of Brain Gray Matter Density and Olfactory Bulb Volume in Patients with Olfactory Loss after Traumatic Brain Injury. J. Neurotrauma 35 (22), 2632–2640.

Hoffman, H.J., Rawal, S., Li, C., Duffy, V.B., 2016. New chemosensory component in the U.S. National Health and Nutrition Examination Survey (NHANES): first-year results for measured olfactory dysfunction. Rev. Endocr. Metab. Disord. 17 (2), 221–240. https://doi.org/10.1007/s11154-016-9364-1.

Huart, C., Rombaux, P., Hummel, T., 2019. Neural plasticity in developing and adult olfactory pathways – focus on the human olfactory bulb. J. Bioenerg. Biomembr. 51 (1), 77–87. https://doi.org/10.1007/s10863-018-9780-x.

Hummel, T., Sekinger, B., Wolf, S.R., Pauli, E., Kobal, G., 1996. "Sniffin" Sticks': Olfactory Performance Assessed by the Combined Testing of Odor Identification Odor Discrimination and Olfactory Threshold. Rhinology 34 (4), 222–226. https://doi.org/10.1093/chemse/22.1.39.

Hummel, T., Urbig, A., Huart, C., Duprez, T., Rombaux, P., 2015. Volume of olfactory bulb and depth of olfactory sulcus in 378 consecutive patients with olfactory loss. J Neurol 262, 1046–1051. https://doi.org/10.1007/s00415-015-7691-x.

Joshi, A., Thaploo, D., Yan, X., Herrmann, T., Khabour, H.A., Hummel, T., Louis, M., 2020. A novel technique for olfactory bulb measurements. PLoS One 15 (12), e0243941.

Karaoglan, M., & Colakoglu Er, H. (2020). Radiological evidence to changes in the olfactory bulb volume depending on body mass index in the childhood. *International Journal of Pediatric Otorhinolaryngology*, *139*(October), 110415. 10.1016/j.ijporl.2020.110415.

Karstensen, H.M., Vestergaard, M., Baaré, W.F.C., Skimminge, A., Djurhuus, B., Ellefsen, B., Brüggemann, N., Klausen, C., Leffers, A.M., Tommerup, N., Siebner, H. R., 2018. Congenital olfactory impairment is linked to cortical changes in prefrontal and limbic brain regions. Brain Imaging Behav. 12 (6), 1569–1582. https://doi.org/10.1007/s11682-017-9817-5.

Kingma, D.P., Ba, J.L., 2015. Adam: A method for stochastic optimization. Published as a Conference Paper at ICLR 2015, 1–15.

Kumar, A., Singh, A., 2015. Pharmacological Reports Review article A review on Alzheimer ' s disease pathophysiology and its management: an update. Pharmacol. Rep. 67 (2), 195–203. https://doi.org/10.1016/j.pharep.2014.09.004.

Litjens, G., Kooi, T., Bejnordi, B.E., Arindra, A., Setio, A., Ciompi, F., Ghafoorian, M., Van Der Laak, J.A.W.M., Ginneken, B.V., Clara, I.S., 2017. A Survey on Deep Learning in Medical Image Analysis. Med. Image Anal. 42, 60–88.

Lötsch, J., Ultsch, A., Eckhardt, M., Huart, C., Rombaux, P., Hummel, T., 2016. Brain lesion-pattern analysis in patients with olfactory dysfunctions following head trauma. NeuroImage Clinical 11, 99–105. https://doi.org/10.1016/j.nicl.2016.01.011.

Lüders, E., Steinmetz, H., Jäncke, L., 2002. Brain size and grey matter volume in the healthy human brain. Neuroreport 13 (17), 2371–2374. https://doi.org/10.1097/00001756-200212030-00040.

Lundström, J.N., Boesveldt, S., Albrecht, J., 2011. Central Processing of the Chemical Senses: An Overview. ACS Chem Neurosci. 2 (1), 5–16. https://doi.org/10.1021/cn1000843.

Marin, C., Vilas, D., Langdon, C., Alobid, I., López-chacón, M., Haehner, A., Hummel, T., Mullol, J., 2018. Olfactory Dysfunction in Neurodegenerative Diseases. Curr. Allergy Asthma Rep. 18 (8), 42. https://doi.org/10.1007/s11882-018-0796-4.

Negoias, S., Pietsch, K., Hummel, T., 2017. Changes in olfactory bulb volume following lateralized olfactory training. Brain Imaging Behav. 11 (4), 998–1005. https://doi.org/10.1007/s11682-016-9567-9.

Nguyen, A.D., Pelavin, P.E., Shenton, M.E., Chilakamarri, P., McCarley, R.W., Nestor, P. G., Levitt, J.J., 2011. Olfactory sulcal depth and olfactory bulb volume in patients with schizophrenia: An MRI study. Brain Imaging Behav. 5 (4), 252–261. https://doi.org/10.1007/s11682-011-9129-0.

Noothout, J.M.H., De Vos, B.D., Wolterink, J.M., Postma, E.M., Smeets, P.A.M., Takx, R. A.P., Leiner, T., Viergever, M.A., Isgum, I., 2020. Deep Learning-Based Regression and Classification for Automatic Landmark Localization in Medical Images. IEEE Trans. Med. Imaging 39 (12), 4011–4022.

Noothout, J.M.H., Postma, E.M., Boesveldt, S., De Vos, B.D., Smeets, P.A.M., Isgum, I., 2021. Automatic segmentation of the olfactory bulbs in MRI. SPIE Medical Imaging 11596–111551.

Oleszkiewicz, A., Schriever, V.A., Croy, I., Hähner, A., Hummel, T., 2019. Updated Sniffin' Sticks normative data based on an extended sample of 9139 subjects. Eur. Arch. Otorhinolaryngol. 276 (3), 719–728. https://doi.org/10.1007/s00405-018-5248-1.

Parma, V., Ohla, K., Niv, M.Y., 2020. More than just smell - COVID-19 is associated with severe impairment of smell, taste, and chemesthesis. Chem. Senses, June. https://doi.org/10.1101/2020.05.04.20090902.

Poessel, M., Breuer, N., Joshi, A., Pampel, A., Villringer, A., Hummel, T., Horstmann, A., 2020. Reduced Olfactory Bulb Volume in Obesity and Its Relation to Metabolic Health Status. Front. Hum. Neurosci. 14 (November), 1–12. https://doi.org/10.3389/fnhum.2020.586998.

Postma, E.M., De Graaf, C., Boesveldt, S., 2020. Food preferences and intake in a population of Dutch individuals with self-reported smell loss: An online survey. Food Qual. Prefer. 79, 103771 https://doi.org/10.1016/j.foodqual.2019.103771.

Rombaux, P., Duprez, T., Hummel, T., 2009. Olfactory bulb volume in the clinical assessment of olfactory dysfunction. Rhinology 47 (1), 3–9.

Rombaux, P., Huart, C., Deggouj, N., Duprez, T., Hummel, T., 2012. Prognostic value of olfactory bulb volume measurement for recovery in postinfectious and posttraumatic olfactory loss. Otolaryngology - Head and Neck Surgery (United States) 147 (6), 1136–1141. https://doi.org/10.1177/0194599812459704.

Rottstaedt, F., Weidner, K., Strauß, T., Schellong, J., Kitzler, H., Wolff-Stephan, S., Hummel, T., Croy, I., 2018a. Size matters – The olfactory bulb as a marker for depression. J. Affect. Disord. 229, 193–198.

Rottstaedt, F., Weidner, K., Hummel, T., Croy, I., 2018b. Pre-aging of the Olfactory Bulb in Major Depression With High Comorbidity of Mental Disorders. Front. Aging Neurosci. 10 (November), 1–7. https://doi.org/10.3389/fnagi.2018.00354.

Sadeghi, M., Amali, A., Ezabadi, S.R., Motiee-Langroudi, M., Farshchi, S., Mokhtari, Z., 2015. Evaluation of the olfactory bulb volume and olfactory threshold in patients with nasal polyps and impact of functional endoscopic sinus surgery: A longitudinal study. International Forum of Allergy and Rhinology 5 (4), 356–360. https://doi.org/10.1002/alr.21478.

Shehata, E.M., Tomoum, M.O., Amer, M.A., Alarabawy, R.A., Eltomey, M.A., 2018. Olfactory bulb neuroplasticity: A prospective cohort study in patients with chronic rhinosinusitis with nasal polyps. Clin. Otolaryngol. 43 (6), 1528–1534. https://doi.org/10.1111/coa.13202.

Thomann, P.A., Dos Santos, V., Toro, P., Schönknecht, P., Essig, M., Schröder, J., 2009. Reduced olfactory bulb and tract volume in early Alzheimer's disease-A MRI study. Neurobiol. Aging 30 (5), 838–841. https://doi.org/10.1016/j.neurobiolaging.2007.08.001.

Tsivgoulis, G., Fragkou, P.C., Lachanis, S., Palaiodimou, L., Lambadiari, V., Papathanasiou, M., Sfikakis, P.P., Voumvourakis, K.I., Tsiodras, S., 2021. Olfactory bulb and mucosa abnormalities in persistent COVID-19-induced anosmia: a magnetic resonance imaging study. Eur. J. Neurol. 28 (1), e6–e8. https://doi.org/10.1111/ene.14537.

Yao, L., Yi, X., Marian, J., Xiandao, P., Yichen, Y., Yifan, G., Yongxiang, L., 2018. Olfactory cortex and Olfactory bulb volume alterations in patients with post-infectious Olfactory loss. Brain Imaging Behav. 12 (5), 1355–1362. https://doi.org/10.1007/s11682-017-9807-7.

Yildirim, D., Altundag, A., Tekcan Sanli, D.E., Bakir, A., Eryurekli, A., Alis, D., Kandemirli, S.G., 2020. A new perspective on imaging of olfactory dysfunction: Does size matter? Eur. J. Radiol. 132 (May), 109290 https://doi.org/10.1016/j.ejrad.2020.109290.

Yousem, D.M., Geckle, R.J., Doty, R.L., Bilker, W.B., 1997. Reproducibility and Reliability of Volumetric Measurements of Olfactory Eloquent Structures. Acad. Radiol. 4 (4), 264–269. https://doi.org/10.1016/S1076-6332(97)80027-X.

Yousem, D.M., Geckle, R.J., Bilker, W.B., Doty, R.L., 1998. Olfactory bulb and tract and temporal lobe volumes: normative data across decades. Ann. N. Y. Acad. Sci. 855 (1), 546–555.